SAND96-1493C
CONF-960805--3 96502

Mass Transport, Corrosion, Plugging, and Their Reduction in Solar Dish/Stirling Heat Pipe Receivers

Douglas R. Adkins, Charles E. Andraka, Robert W. Bradshaw, Steven H. Goods,
James B. Moreno, and Timothy A. Moss
Sandia National Laboratories
P. O. Box 5800, MS 0835
Albuquerque. NM 87185
Phone (505) 844-0611, FAX (505) 844-8251

ABSTRACT

Solar dish/Stirling systems using sodium heat pipe receivers are being developed by industry and government laboratories here and abroad. The unique demands of this application lead to heat pipe wicks with very large surface areas and complex three-dimensional flow patterns. These characteristics can enhance the mass transport and concentration of constituents of the wick material, resulting in wick corrosion and plugging. As the test times for heat pipe receivers lengthen, we are beginning to see these effects both indirectly, as they affect performance, and directly, in post-test examinations. We are also beginning to develop corrective measures. In this paper, we report on our test experiences, our post-test examinations, and on our initial effort to ameliorate various problems.

INTRODUCTION

Through joint-venture programs with several industrial partners, the Department of Energy is sponsoring programs to commercialize solar-to-electric power generating systems that use parabolic mirror solar concentrators coupled with a Stirling engine and generator. One of the major challenges of this program is to develop a solar receiver system to transfer energy from the focus of the concentrator to the working fluid of the engine. Flux levels near the focus can be on the order of 100 W/cm^2 and, depending on the quality of the concentrator, the flux distribution on the receiver can be very non-uniform. In earlier solar/Stirling systems, tubes transporting the engine's working fluid were directly heated with concentrated solar energy. This practice created large thermal gradients on the tubes and led to concerns about the life expectancy of direct-receiver systems. The uneven flux profiles on the receiver also led to problems in achieving a balanced thermal input in multi-cylinder engines.

Heat-pipe solar receivers are currently being developed as an alternative to directly-illuminated tube receiver systems. Figure 1 illustrates the operation of the receiver. A wick structure distributes sodium across a solar-heated dome, and thermal energy is removed from the dome as the sodium evaporates. Sodium vapor condenses on the heater tubes of the engine where the energy is transferred to the engine's working fluid (typically helium). Condensed liquid then flows back to the wick-covered evaporator surface under the influence of gravity. The geometry of a receiver is tailored to the concentrator's power distribution and a receiver's operating characteristics. In the current systems, input powers are as high as 75 kW and receiver domes are nominally 16-inch (41-cm) diameter hemispheres. Andraka et al. [1996] provides a comparison of performance between a heat-pipe receiver and a directly illuminated tube system.

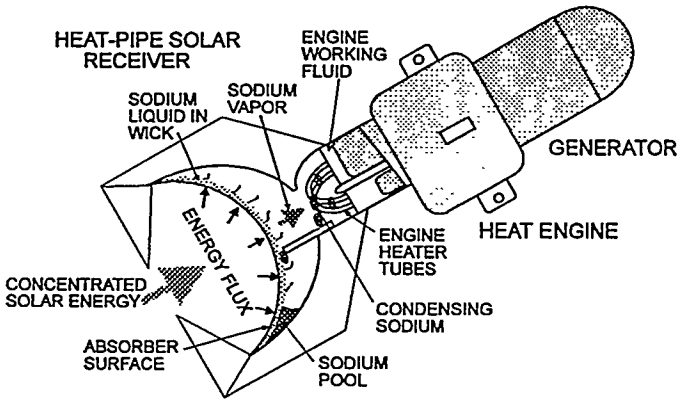

Figure 1. Operating schematic of a heat pipe solar receiver.

This work was performed at Sandia National Laboratories, supported by the U. S. Department of Energy under contract number DE-AC04-94AL85000

Metal felts are being used as wick structures in several of the heat-pipe receivers that are now under development. Felts that are made of micron-diameter wires can have porosities greater than 90% and, in an unsintered state, the materials are very pliable, so they can be shaped to fit the absorber dome. It is also possible to modify the pore structure by compacting or expanding the material. Adkins et al. [1995] presents permeability and pore-size data on felt materials, and Andraka et al. [1995] models the flow of liquid through the felt-metal wick structures and predicts the performance limits of the receiver system.

Metal felts are most commonly used in filter applications, but they have been used in heat pipe systems in the past. Davis and Ferrell [1974] found that a potassium heat pipe system with a stainless steel felt wick could operate at about 600°C with flux levels of up to 31 W/cm^2. It also has been found that stainless steel felt wicks can operate in liquid metal environments for long periods at elevated temperatures. Ewell et al. [1978] found only a small amount of grain boundary relief in a stainless steel felt wick after 2300 hours of operation in sodium at 700°C. After 10,000 hours of operation, Ewell et al. reported increased grain boundary relief and fracturing where some of the fibers were bent. However, they predicted that the wick should easily be able to withstand 50,000 hours of operation.

In spite of these earlier findings, the long-term viability of felt-metal wick materials continues to be an area of concern. Current receiver systems are intended to operate at 750°C, and the fibers in these systems are 4 μm in diameter as compared to the 10 μm fibers in the studies of Ewell et al.. Higher temperatures and smaller fiber size will exacerbate corrosion problems. The high heat fluxes and large surface areas will also lead to increased concentrations of sodium oxides and corrosion products in the evaporator region of the heat pipe. While it is recognized that cleaning and other preparations may mitigate these effects, there is also the need to minimize the preparation procedures in order to create a cost-effective receiver system.

To gain a better understanding of the operating life issues, Sandia National Laboratories has undertaken an effort to systematically study corrosion problems in sodium heat-pipe systems and the corresponding influence of cleaning techniques. Results from a recent bench-scale receiver system are provided below along with a review of our current understanding of this area and a discussion of future sodium heat-pipe corrosion studies at Sandia.

BENCH-SCALE RECEIVER SYSTEM

Construction

A schematic of the bench-scale receiver system is illustrated in Figure 2. The envelope of the receiver is made of a nickel-based super alloy (Haynes 230) which has been selected for full-scale receiver applications because of its high strength and air-side corrosion resistance at elevated operating temperatures. The wick material is a 316L metal fiber that is sold by Bekaert Fibre Technologies as Bekipor® WB 04/150, where 04 refers to the wire diameter (4 μm) and 150 refers to the mass of one square meter of the material (150 g/m^2). The nominal composition of 316L stainless steel and Haynes 230 alloy are shown in Table 1 and Table 2 respectively.

Two layers of the felt metal were attached to each curved wall of the heat pipe by sintering in a hydrogen furnace for one hour at 1150°C. After sintering, the felt wick was compacted to 4.7-mm thick, and then the walls were gas-tungsten-arc (GTA) welded together to form the heat pipe envelope. An argon purge was maintained during the GTA welding process. After the GTA weld, the sides were electron-beam welded under vacuum to achieve full weld penetration along the edges. The heat pipe was 22" (559-mm) long and it had a 2.25" x 1.00" (57.2-mm x 25.4-mm) rectangular cross-section in the middle and a 2.25" x 3" (57.2-mm x 76.2-mm) rectangular cross-section at the ends. A fan-folded strip of zirconium was attached at the bottom of the heat pipe in the pool area to act as a getter.

Prior to charging with sodium, the heat pipe was vacuum baked at 700°C for 4 days. A charge of 500 g of sodium was added to the heat pipe, and the pipe was laid on its side and heat soaked at 400°C for about 3 hours to wet the wick. After the filling and priming process, the heat pipe was mounted vertically in a stand for high flux testing. An array of quartz lamps was used to heat a 42-mm x 102-mm area on the surface of the heat pipe. The average flux into the heated area was approximately 60 W/cm^2. The operating temperature was controlled by circu-

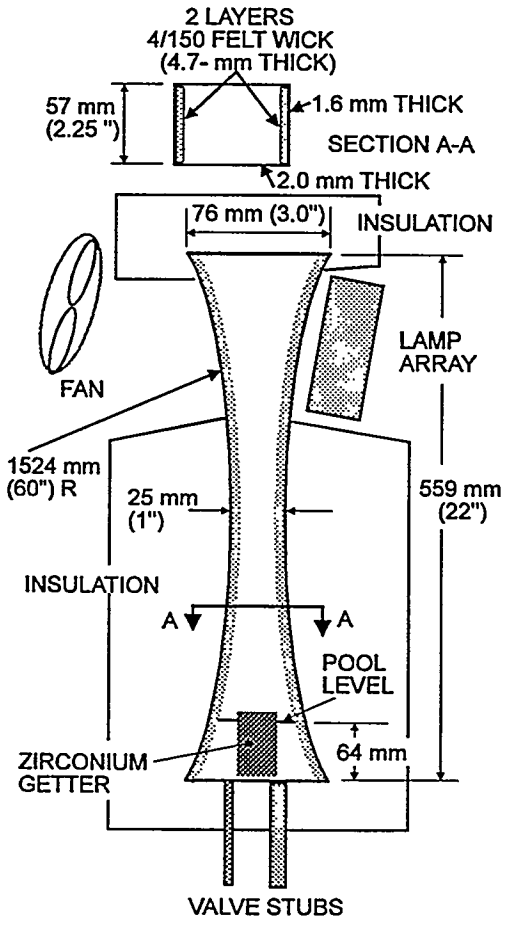

Figure 2. Schematic of the bench-scale receiver system.

Table 1. Nominal Composition of 316L Stainless Steel (weight %).

Fe	Ni	Cr	Mo	Si	Mn	C (max)
bal (≈64)	10-14	16-18	2-3	1 (max)	2	0.03

Table 2. Nominal Composition of Haynes 230. B, Cu, P, S, Ti, and V are present at levels less than 0.02% (weight %).

Fe	Ni	Cr	W	Mo	Si	Mn	C	Al	Co
3.0 max	bal (≈60)	20-24	13-15	1-3	0.75 max	0.3-1	0.15 max	0.5 max	5.0 max

lating air across an uncovered wall of the heat pipe (opposite the lamps) with a thermostatically controlled fan. Temperatures were measured with intrinsic thermocouples welded to the surface of the heat pipe.

Operation

At the operating temperature of 750°C, the pool was approximately 64 mm (2.5") deep. The lamps were 51 mm (2") from the top of the receiver, and, since most of the condensation occurred on the side opposite the lamps, the liquid was required to flow about 444 mm (17.5") to reach the top of the heated area. The total power throughput was on the order of 2600 W.

After operating 1995 hours, a hot spot developed on the surface near the top of the heated region. The overheat occurred when the system was restarted after an unrelated shutdown. Temperatures near the top of the heated region rose uncontrollably when power was applied to the lamps, and a heavily oxidized area appeared on the surface.

Sodium was distilled at 600°C from the system into a drain can. Afterwards, the system was milled open and sectioned. Near the top of the evaporator region, the wick was eaten through to the substrate and a white residue was on the surface. About 1 cm below this hole in the wick, a thin stripe of copper appeared, and many other deposits could be observed in the wick structure with a microscope. A black deposit was present in the pool area, and a strong sulfur smell emanated from the heat pipe after it was opened.

Post Mortem

The system was opened and sectioned for post-mortem analysis. While the analysis is still in progress, we can report on a number of preliminary observations. A variety of microstructural and compositional changes were observed in the wick depending upon the particular location within the heat pipe. The structure of the wick was examined using scanning electron microscopy. Energy dispersive spectroscopy (EDS) was used to determine the composition of corrosion products.

Near the top of the evaporator region, the thickness of the wick was considerably reduced. A small "crater" measuring several millimeters in diameter, was also observed in this region. Associated with this crater was evidence of the formation of oxides containing the primary constituents of stainless steel as well as sodium. The crater penetrated to the Haynes alloy substrate and was the result of the nearly complete corrosion or dissolution of the wick fibers.

Nodules deposited on the evaporator wick structure showed a high concentration of oxygen and calcium (see point A in Figure 3). An analytical report provided with the high-purity sodium used in charging the heat pipe indicates that calcium was present at a concentration of 13 ppm. The report also indicated that oxygen levels were less than 10 ppm. Other, smaller deposits on the stainless steel fibers can also be seen (point B, for example). As shown in the Table in Figure 3, the composition of the corrosion product at point B is complex, containing both the constituents of stainless steel as well as oxygen, aluminum (a minor constituent of Haynes 230) and sodium. The composition of Haynes 230 and the nominal composition of 316L are shown in Table 1 and Table 2. The copper deposit on the evaporator surface could have come from the Haynes alloy, or it may have been introduced with the felt wick. (Copper sleeves are apparently used at some point of the felt fabrication process.)

Wick fibers located immediately below the evaporator showed evidence of preferential grain boundary attack and significant thinning. As a result, the fibers have a scalloped appearance as can be seen in Figure 4. An EDS analysis of these fibers indicates that exposure to sodium resulted in a modification of the surface composition of the 316L from that of the as-received felt. Some surface features (i.e., Region A, Figure 4) showed elevated chromium levels while much of the general surface (i.e., Region B) retains the nominal composition of 316L stainless steel. Oxides were not generally found in this location.

Wick material extracted from the condenser section showed some dissolution and corrosion although the attack was less pronounced than was observed in the evaporator area. Regions marked A in Figure 5 identify locations of surface faceting of the fibers. These sites are characteristically low in iron and nickel, and they appear to have formed by the preferential dissolution of these constituents. Higher than normal concentrations of molybdenum were also observed at the faceted sites. Sites containing both oxygen and aluminum were also identified (Region B); however, away from these features (Region C for example), the general fiber surfaces exhibit the nominal composition of the as-received felt alloy.

The black deposits in the pool area were found to have zirconium, nickel and oxygen as the primary constituents. An examination of the wick from the pool region of the heat pipe revealed the presence of deposits on most of the metal fiber surfaces. Figure 6 shows the characteristic morphology of these deposits and EDS analysis indicated that they were metallic, consisting of the elemental constituents of stainless steel with a very high concentration of chromium. Away from the nodules, the composition of the pool wick material correlated fairly well with the standard constituents of 316L listed in Table 1.

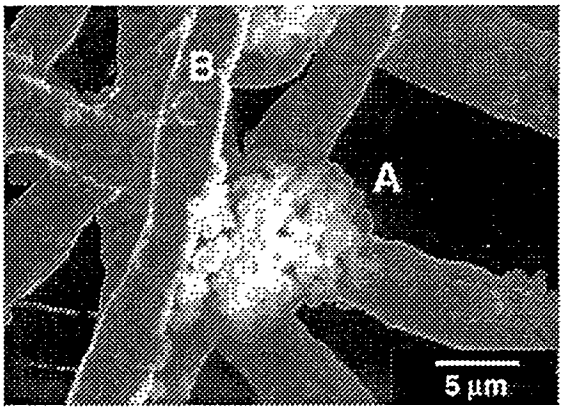

Region	Fe	Cr	Ni	O	Al	Ca	Na
A	2.0	2.5	0.5	28.8	0.0	63.8	1.1
B	29.3	8.3	7.7	17.3	16.7	0.7	18.5

Figure 3. Scanning electron micrograph showing the structure of the wick in the evaporator region. Formations of compounds containing calcium and oxygen were abundant in this area. Deposits of sodium compounds were also present.

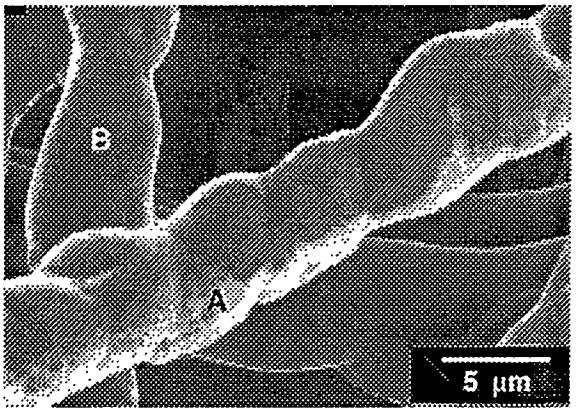

Region	Fe	Cr	Ni	Mo
A	39.4	48.3	3.2	8.3
B	74.0	10.7	13.3	0.8

Figure 4. Wick structure below the evaporator region. This material was in the path of the liquid sodium flowing to the heated area. Accompanying table in wt. %.

DISCUSSION OF RESULTS

Two mechanisms contribute to the dissolution or corrosion of materials in liquid sodium systems: (1) Metallic element mass transfer where solid metals dissolve into the liquid sodium and are transported away, and (2) Non-metallic element mass transfer where alloys and chemical compounds are formed [Natesan, 1975]. Much of the work on metal corrosion in liquid metal environments is summarized in Volume 1 of the Sodium NaK Engineering Handbook [Foust, 1972]. Both Foust and Natesan, however, present results where sodium is present only in the liquid state. Evaporation and condensation within a heat

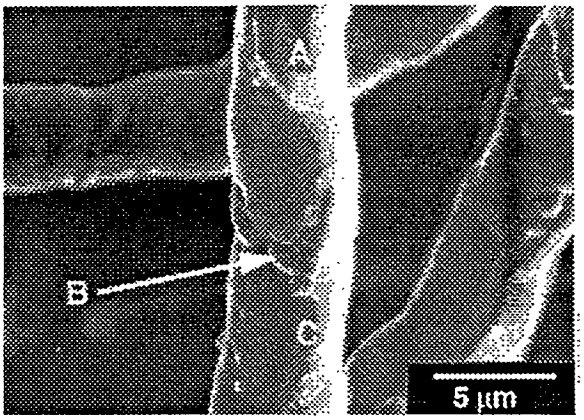

Region	Fe	Cr	Ni	Mo	O	Al
A	44.2	21.6	2.8	27.3	-	-
B	57.7	11.6	8.0	1.5	12.9	7.4
C	71.7	15.1	10.9	0.8	-	-

Figure 5. Structure of the wick on the condenser surface.

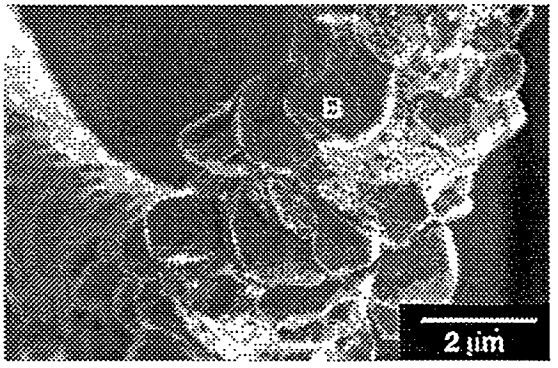

Region	Fe	Cr	Ni	Mo
B	25.2	66.7	6.4	1.7

Figure 6. Nodule formation on the wick structure in the pool area.

pipe works to concentrate contaminants, and these concentrating effects can be large. With an average flux level of 60 W/cm^2, about 54 g of sodium evaporates from a square centimeter of the heated zone every hour. The total liquid flow rate through the evaporator wick was 2300 g/hr. Over the course of 2000 hours of operation, even 10 ppm levels of contaminant concentration could leave behind a gram of residue on each square centimeter of the evaporator surface.

Oxygen contamination in the sodium is known to increase the solubility of metals in sodium and accelerate corrosion effects. The large surface area of the wick, and the ineffectiveness of the current cleaning techniques in removing native oxide layers most likely contributed to a high concentration oxygen in the sodium. The influence of oxygen concentration on the dissolution process of iron and nickel based alloys is attributed to the formation of sodium ferrates and sodium chromates, and the subsequent

dissolution or erosion of these compounds [Horsley, 1956]. Natesan indicated that corrosion rates of 10 μm per year were possible in 750°C flowing sodium with oxygen concentrations as low as 5 ppm. (This corrosion rate was based on a liquid flowrate of 3 m/s. In our heat pipe, the liquid velocity was much lower, more on the order of 3.5 mm/s, but the oxygen content was probably higher.)

The oxygen concentration in the sodium can be estimated knowing the mass of sodium in the wick and the thickness of the native oxide on the wick surface. Sodium fills the voids in the wick material, and the void fraction or porosity of the material is given by the expression

$$\varepsilon = 1 - \frac{\delta_f}{\delta}, \qquad (1)$$

where δ is the thickness of each layer of the wick material, and δ_f is the equivalent thickness of the wick material if it is compressed to zero porosity. If the material has a weight per square meter of B and the wire fibers have a density ρ, then the equivalent thickness $\delta_f = B/\rho$. For 4/150 felt, $\delta_f = 19.2$ μm, and for 8/300 felt $\delta_f = 38.4$ μm. The surface area per square meter of felt wick is

$$S = \frac{4\delta_f}{D}, \qquad (2)$$

where D is the wire diameter. According to this calculation, a single layer of 4/150 felt metal has about 19 m^2 of surface area per square meter of fabric. If the native oxide on the felt wires is assumed to be chromium-oxide (Cr_2O_3) with a thickness δ_{OXIDE}, then the oxygen concentration in the sodium saturated wick will be

$$C = \frac{3}{\varepsilon}\frac{S}{\delta}\frac{\delta_{CR2O3}}{MW_{CR2O3}}\frac{MW_O}{\rho_{Na}}\rho_{CR2O3}, \qquad (3)$$

when the system is first primed. Auger analysis of the felt wick showed that the native oxide layer was on the order of 5 nm thick, so the two layers of 4/150 felt that were compacted to about 4.7 mm thick in the test pipe could have brought the oxygen level in the sodium up to about 85 ppm by weight. Other factors, such as the thermodynamics of the sodium and chromium-oxide reaction, and the diffusion rate of oxides into solution, will limit the oxygen concentration

The actual solubility of oxygen in sodium is a function of temperature as Figure 7 illustrates. At 160°C, the solubility of oxygen is less than 3 ppm, and at 500°C the maximum solubility of oxygen in sodium is 1200 ppm. Temperatures within the heat pipe were fairly uniform at 750°C, so the liquid never would have reached the saturation limit for oxygen. Even in the pool where the temperature was on the order of 600°C, the oxygen would have remained in solution.

An exact mechanism for our systems failure is unknown at this point, but, based on our understanding of the corrosion processes in liquid metals and the post mortem results, we can assemble a reasonable failure scenario. The corrosion process begins as sodium vapor condenses on the cooled condenser surface. The condensed sodium is fairly pure, so oxygen from the chromium oxide layer on the wick surface would readily go into solution. As the oxygen contaminated sodium flows down the condenser wick to the pool, elemental constituents of the wick material begin to go into solution. Chromium is known to have a fairly high solubility in oxygen-contaminated sodium, and iron is also soluble, but slightly less so [Foust, 1972]. (The solubility of nickel in oxygen-contaminated sodium is uncertain, and results provided by Foust are contradictory.)

Condensed sodium flows to the pool, and the liquid cools, causing some of the metals to come out of solution. Some of the oxygen in the sodium is gettered by the zirconium, but the process is diffusion limited. Liquid sodium from the pool, which is still contaminated with oxygen, is transported by capillary pumping through the wick structure to the evaporator surface. As the liquid flows to the evaporator surface, oxygen and other material from the wick structure goes into solution and gets transported to the evaporator area. Liquid sodium evaporates away in the heated area and leaves behind the metals that were pulled into solution and the oxide compounds with low vapor pressures. The metallic residues begin to collect in the evaporator wick structure and block the flow of liquid sodium. Oxide compounds are gradually swept to the top of the evaporator section where they concentrate. Eventually, the concentrated oxide compounds corrode away a section of the wick, and, without a supply of liquid sodium, the surface previously attached to the destroyed wick overheats. The sulfur smell that was present when the system was cut open probably indicates that trace amounts of sulfur in the material had combined with hydrogen that was released from the walls during the vacuum bakeout and the operation of the heat pipe.

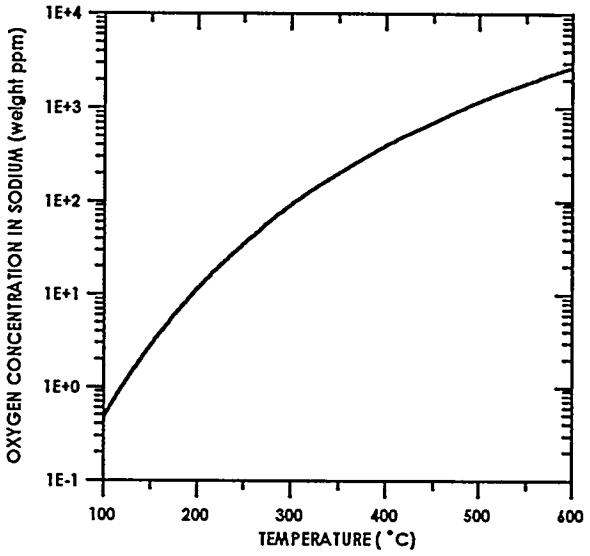

Figure 7. Solubility of oxygen in sodium as a function of temperature [Foust, 1972].

CORROSION MITIGATION EFFORTS

Corrosion mitigation techniques are still under development in this program, so a final solution is not available. Some findings from this effort, however, are worthy of mention. The main goal of any of the cleaning/processing techniques is to reduce the native oxide layer on the interior heat pipe materials in order to minimize the oxygen concentration in the liquid-metal working fluids.

One of the more common practices in heat-pipe processing is to vacuum bake the system at a temperature greater than the eventual operating temperature of the system. This practice will reduce the evolution of gases at the operating temperature, but it will not necessarily reduce the oxide layers on the interior surface. According to information published by the American Welding Society [1976], iron oxides and nickel oxides readily reduce at temperatures above 100°C and pressures below 10^{-2} Pa, but temperatures above 600°C are required to reduce Cr_2O_3 at this pressure. The rate of reduction at this temperature is not specified, and it is also noted that lower temperatures can actually contribute to oxidation of the material if the partial pressure in the system is primarily due to water vapor. Los Alamos National Laboratories typically used vacuum bake-out temperatures above 900°C for their liquid metal heat pipes [Merrigan 1996].

An alternative to increasing the bakeout temperature is to use the sodium to clean the oxides off of the interior surfaces. Stelman and Newcomb [1993] describe performing multiple sodium rinses on heat pipes to drive oxygen concentration levels down to 8 ppm. In their system, sodium from a large reservoir circulates in a loop with a cold-trap where oxides are removed by filtration after they precipitate out of solution. Heat pipes are filled and drained on a second loop connected to the reservoir. According to Stelman and Newcomb, the heat pipes are vacuum baked at 427°C, and then filled with sodium and heat soaked at 427°C for 24 hours. After the heat soak, the heat pipe was drained and flushed with hot sodium for 48 hours. This process of filling, heat soaking, and finally flushing was repeated a minimum of three times. In addition to the cold trap, Stelman and Newcomb's system also used a molecular sieve followed by a hot zirconium getter and a particle filter to further reduce contaminants in the liquid sodium.

Condensing pure sodium on the internal surfaces of the heat pipe and allowing the liquid to carry away the contaminants is another cleaning process that has been investigated. Our initial attempt at this procedure appears to have been unsuccessful though. A heat pipe similar to the above bench-scale system was vacuum baked at 600°C, and then sodium was allowed to distill at 600°C from a stainless steel vessel at the base of the heat pipe. Sodium from the vessel condensed at 550°C on the interior surface of the heat pipe and then flowed back to the distillation vessel. This reflux-cleaning process was allowed to continue for about 6 hours before the final charge from the distillation vessel was distilled back into the heat pipe. The heat pipe operated for about 1300 hours before it too developed a hot spot. A post mortem analysis has not yet been performed, but it is suspected that the same failure mechanism as the first pipe was repeated.

It is possible that reflux cleaning did not work because oxygen was being re-introduced into the system through some vapor transport mechanism. Ivanovsky, Morozov, and Shimkevich [1995] indicate that distillation/condensation cleaning methods are ineffective because a "fine system of complex compounds is volatile." The precise meaning of this statement is unknown, but Ivanovsky implies that the sublimation of compound colloids (such as collodial solution of sodium chromate) and the transfer of compound colloids by wet vapor droplets plays a major role in transporting oxygen in heat pipes. It may be possible to eliminate the colloidal mixtures in cold traps; however, Ivanovsky warns that the crystallization required for cold trapping proceeds slowly.

At this time, a definitive procedure for cleaning and filling heat pipes in an economical way has not been found. It is also unclear what level of oxygen concentration could be considered acceptable since the operation of the heat pipe tends to concentrate corrosive oxides in the evaporator wick. An effort is now underway to establish capsule tests to explore the effectiveness of various cleaning techniques.

CONCLUSIONS

The Department of Energy and several industrial partners are currently engaged in programs to develop heat-pipe systems to transport solar-thermal energy from the focus of a parabolic mirror to the heater tubes of a Stirling engine. These heat-pipe solar-receiver systems are intended to operate for 90,000 hours with little or no maintenance. The lifetime of the receivers systems is highly dependent on the purity of the sodium working fluid of the heat pipe. One of the major sources of contamination in the heat pipe is the native oxide layer on the interior surface of the heat pipe. In particular, the high surface area of the felt-metal wick that is being developed in this program greatly increases the oxygen introduced into the heat pipe through native oxide layers.

The operating characteristics of a heat pipe will tend to concentrate damage in the evaporator section of the heat pipe. High heat flux levels and operating temperatures contribute to the rapid deterioration of the current systems. For the sodium heat-pipe system described in this paper, the greatest dissolution and corrosion of the wick occurred in the evaporator section. Deposits of materials in the evaporator wick structure also contributed to the failure of the system after 1995 hours of operation. The removal of material was also observed in the wick structure below the evaporator section. This area would have been subjected to a flow of liquid sodium with a high concentration of oxygen contamination. The wick structure was attacked to a lesser extent in the condenser region.

Efforts to mitigate the corrosion effects are still under development. There is some indication that the oxygen cannot be removed through simple distillation processes. It may be possible to improve the reduction of the native oxide layers with a higher temperature (greater than 900°C) vacuum bake out. A series of capsule tests is now underway to determine a cost-effective system for processing liquid metal heat pipes.

REFERENCES

Adkins D., Moss, T., Andraka, C., Cole, H., Andreas, N., 1995, "An Examination of Metal Felt Wicks for Heat-Pipe Applications," ASME/JSME Solar Engineering Conf., Maui, HA.

American Welding Society, 1976, *Brazing Manual*, 3rd ed., American Welding Society, 2501 N.W. 7th Street, Miami, FL 33125.

Andraka C., Rawlinson, K., Moss, T., Adkins D., Moreno, J., Gallup, D., Cordeiro, P., 1996, "Solar Heat Pipe Testing of the Stirling Thermal Motors 4-120 Stirling Engine," Proceedings of the 31st IECEC, Washington, D.C..

Andraka, C., Adkins, D., Moss, T., Cole, H., Andreas, N., 1995, "Felt-Metal-Wick Heat-Pipe Solar Receiver," ASME/ JSME Solar Engineering Conf., Maui, HA.

Davis, W.R., and Ferrel, J. K., 1974, "Evaporative Heat Transfer of Liquid Potassium in Porous Media," *Proceedings of AIAA/ASME Thermophysics and Heat Transfer Conference*, paper no. 74-719, Boston, MA, July 15-17.

Ewell, G. J., Basiulis, A., and Lamp, T. R., 1978, "Reliability of Low-Cost Liquid Metal Heat Pipes," *Proceedings of the Third International Heat Pipe Conference*, Palo Alto, CA, May 22-24.

Foust, O. J., ed.,1972, *Sodium-NaK Engineering Handbook, Volume I, Sodium Chemistry and Physical Properties*, Gordon and Breach, Science Publishers, Inc., 440 Park Ave. So., New York, NY.

Horsley, G. W., *J.*, 1956, *Iron Steel Inst.*, Vol. 182, no. 1, p. 43.

Ivanovsky, M. N., Morozov, V. A., and Shimkevich, A. L., 1995, "On Advanced Technology of Fluids for Heat Pipes," *Proceedings of the IX International Heat Pipe Conference*, Albuquerque, NM.

Merrigan, M., 1996, personnel communication.

Natesan, K., 1975, "Interactions Between Structural Materials and Liquid Metals at Elevated Temperatures," *Metallurgical Transactions A*, Vol. 6A, pp. 1143-1153.

Phillips, E.C., and J.D. Hinderman, 1969, "Determination of Properties of Capillary Media Useful in Heat Pipe Design," *Proceedings of the ASME-AICHe Heat Transfer Conf.*, Paper No. 69-HT-18, Minneapolis, MN.

Stelman, D., and J. C. Newcomb, 1993, "Filling and Sealing Sodium Heat Pipes," CONF 930103, Am. Inst. of Physics, pp. 533-538.

DISCLAIMER